Appendix 1

The process for quantitative airway geometrical analysis

All chest CT images used for airway geometric analysis were acquired with the following technical parameters: detector collimation of 1.25–0.625 mm, tube voltage of 120 kVp, tube current of 150–200 mA, and a reconstruction interval of ≤1 mm. These acquisition settings were applied to ensure adequate spatial resolution for subsequent quantitative airway morphometric analysis. All scans were performed in a tertiary referral hospital setting as part of routine diagnostic evaluation, prior to bronchoscopy procedures.

For quantitative assessment of airway geometrical characteristics, we obtained a patient airway mask by segmenting the lung CT image. The target lesion was automatically delineated and subsequently verified by an expert thoracic radiologist (HY Lee) with 18 years of experience in chest imaging. Tumor lesions at different locations were drawn as separate candidates for analysis. All segmentation processes were conducted using commercial deep-learning software (AVIEW; Coreline Soft, Seoul, Korea) and modified manually in cases of inaccurate airway or lesion delineation. Next, both the extracted airway mask and the volumes of interest for the target lesions were entered into in-house software (AirGeo program) to quantify the airway geometrical features. This software remodeled the three-dimensional radial probe pathway from the trachea to each target lesion by emulating the rEBUS-TBLB interventions used in clinical practice. The source code of the AirGeo program is publicly available at https://github.com/Hwan-ho/AirGeo.

We determined morphological characteristics of the airway at every branch level from the trachea to each target lesion. From the perspective of the lung airway lumen, airway morphometry was extracted as follows: sectional area, minimum and maximum diameter, min–max diameter ratio, and perimeter. The circularity of the airway cross-sectional plane perpendicular to the airway centerline direction was also measured and called the *maximum inscribed sphere R*. The luminal circularity and hydraulic luminal diameter were measured as well. The bronchial tubular structure was characterized as two geometrical features reflecting the mechanical properties of the airway: curvature and torsion (distortion). The extracted features were represented using minimum, maximum, and average values at all centerline points. Additionally, we calculated the bifurcation angle at the junction points between branches. A comprehensive description of the computed geometric features can be found in

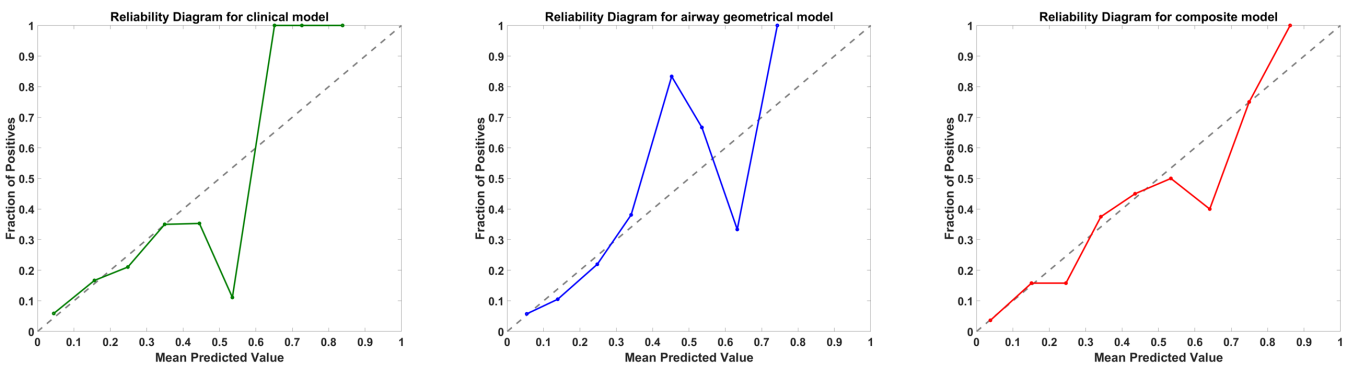

Figure S1 Calibration plot for each proposed model. A calibration graph was obtained by plotting the observed versus predicted probabilities. An ideal nomogram would show a localized regression plot that perfectly fit the 45-degree reference line (dashed line) when the actual versus predicted probability was plotted.

https://dx.doi.org/10.21037/tlcr-2026-1-0133

Table S1 Descriptions of the quantitative airway geometrical features

Feature name	Equation	Description
Area (LA)		Cross-sectional area at the specific centerline point
MaxInscribedSphereR		Radius of 3D maximum inscribed sphere in the airway at the specific centerline point
MinDiameter (D_{min})		Minimum diameter of the cross-sectional plane
MaxDiameter (D_{max})		Maximum diameter of the cross-sectional plane
MinMaxDiameterRatio	$\frac{D_{min}}{D_{max}}$	Ratio of MinDiameter and MaxDiameter
Curvature (κ)	$\kappa = \left\|\frac{dT}{ds}\right\|$, where T is the tangent vector of the airway central line, and s is the distance between centerline points	Curvature of the centerline
Torsion (τ)	$\tau = -n \cdot b'$, where $n = \frac{T'}{\kappa}$ and $b = T \times n$	Torsion of the centerline
Perimeter (P_e)		Perimeter of the cross-sectional plane
LuminalCircularity (C_r)	$C_r = \pi \frac{\sqrt{\frac{4LA}{\pi}}}{P_e}$	Luminal circularity of each centerline point
HydraulicLuminalDiameter (D_h)[1]	$D_h = \frac{4LA}{P_e}$	Airway narrowing

Table S2 Procedural outcomes and diagnostic results according to bronchoscopic accessibility to PPNs

Variables	Total cases (N=219)	Easily accessible (N=182)	Difficult or inaccessible (N=37)	p
Procedure time, min	10.5 ± 6.2	9.4 ± 5.0	15.8 ± 8.7	<0.001
Radial probe positioning during the procedure				<0.001
Within	179 (81.7%)	162 (89.0%)	17 (45.9%)	
Adjacent	29 (13.2%)	20 (11.0%)	9 (24.3%)	
Invisible	11 (5.0%)	0	11 (29.7%)	
Pathologic diagnosis				<0.001
Malignancy[a]	126 (57.5%)	119 (65.4%)	7 (18.9%)	
Benignancy[b]	20 (9.1%)	17 (9.3%)	3 (8.1%)	
Non-diagnostic[c]	57 (26.0%)	46 (25.3%)	11 (29.7%)	
Failed to obtain tissue	16 (7.3%)	0	16 (43.2%)	

[a] Malignancy was confirmed by the presence of malignant cells in the obtained tissue. [b] Benignancy was defined as the presence of definitive pathological features of benign diseases, such as granulomatous inflammation, specific infections (e.g., tuberculosis or fungi), organizing pneumonia, or benign neoplasms (e.g., hamartoma). [c] Non-diagnostic was defined as biopsies that did not meet the criteria for malignancy or any of the aforementioned specific pathological criteria. This category includes biopsies showing only normal lung parenchyma, atypia not diagnostic of malignancy, and nonspecific inflammation. These criteria follow standardized diagnostic definitions for peripheral lung lesions as outlined in recent clinical guidelines (29).

https://dx.doi.org/10.21037/tlcr-2026-1-0133

Table S3 Univariable analysis for airway geometrical features associated with difficult or inaccessible PPNs

	Variables	OR (95% CI)	P
Total branches	Total sectional length, mm	0.820 (0.569–1.182)	0.284
	Total Sum of bifurcation angle-in, degree	1.505 (1.057–2.145)	0.023
	Total Min of bifurcation angle-in, degree	1.223 (0.862–1.736)	0.257
	Total Max of bifurcation angle-in, degree	1.595 (1.086–2.344)	0.017
	Total Average of bifurcation angle-in, degree	1.636 (1.147–2.333)	0.006
	Total SD of bifurcation angle-in, degree	1.362 (0.968–1.916)	0.075
Previous branch to final branch	Sectional length, mm	0.708 (0.467–1.072)	0.101
	Bifurcation angle-in, degree	1.304 (0.925–1.836)	0.127
	Min sectional area, mm^2	1.090 (0.782–1.520)	0.608
	Max sectional area, mm^2	1.163 (0.870–1.555)	0.305
	Average sectional area, mm^2	1.043 (0.739–1.472)	0.809
	Min of max inscribed sphere R, mm	0.887 (0.607–1.297)	0.534
	Max of max inscribed sphere R, mm	0.794 (0.522–1.208)	0.278
	Max of min diameter, mm	0.975 (0.678–1.403)	0.891
	Max of max diameter, mm	1.223 (0.893–1.675)	0.208
	Min of min–max diameter ratio	0.641 (0.435–0.943)	0.023
	Max of min–max diameter ratio	0.931 (0.660–1.313)	0.684
	Average of min–max diameter ratio	0.850 (0.600–1.205)	0.359
	Max curvature, mm^{-1}	0.951 (0.663–1.364)	0.786
	Average curvature, mm^{-1}	1.033 (0.723–1.475)	0.858
	Min torsion, mm^{-1}	1.133 (0.745–1.727)	0.556
	Max torsion, mm^{-1}	0.966 (0.664–1.406)	0.856
	Average torsion, mm^{-1}	1.084 (0.754–1.506)	0.716
	Min perimeter, mm	0.974 (0.678–1.400)	0.888
	Max perimeter, mm	1.066 (0.754–1.506)	0.716
	Min luminal circularity	0.867 (0.614–1.225)	0.417
	Max luminal circularity	0.972 (0.676–1.399)	0.879
	Average luminal circularity	0.949 (0.661–1.363)	0.777
	Max hydraulic luminal diameter, mm	1.013 (0.713–1.439)	0.942
	Average hydraulic luminal diameter, mm	0.987 (0.688–1.416)	0.944
Final branch	Sectional length, mm	1.259 (0.896–1.767)	0.182
	Bifurcation angle-in, degree	1.358 (0.979–1.885)	0.065
	Min sectional area, mm^2	0.653 (0.364–1.172)	0.151
	Max sectional area, mm^2	1.017 (0.716–1.444)	0.924
	Average sectional area, mm^2	0.696 (0.411–1.177)	0.174
	Min of max inscribed sphere R, mm	0.697 (0.477–1.017)	0.060
	Average of max inscribed sphere R, mm	0.623 (0.419–0.928)	0.019
	Max of min diameter, mm	0.896 (0.615–1.306)	0.565
	Min of min–max diameter ratio	0.966 (0.676–1.380)	0.848
	Max of min–max diameter ratio	1.218 (0.789–1.882)	0.371
	Average of min–max diameter ratio	1.308 (0.887–1.931)	0.173
	Max curvature, mm^{-1}	1.512 (1.068–2.141)	0.019
	Average curvature, mm^{-1}	1.474 (1.027–2.115)	0.034
	Min torsion, mm^{-1}	0.976 (0.693–1.376)	0.891
	Max torsion, mm^{-1}	1.061 (0.777–1.449)	0.708
	Average torsion	1.226 (0.858–1.754)	0.261
	Min perimeter, mm	1.167 (0.876–1.554)	0.290
	Max perimeter, mm	0.889 (0.633–1.250)	0.497
	Min luminal circularity	0.388 (0.127–1.182)	0.094
	Max luminal circularity	1.132 (0.787–1.629)	0.501
	Average luminal circularity	0.712 (0.483–1.051)	0.086
	Max hydraulic luminal diameter, mm	0.349 (0.127–0.960)	0.040
	Average hydraulic luminal diameter,mm	0.496 (0.294–0.834)	0.008

Univariable analysis was conducted using the selected airway geometrical features and assessed for multicollinearity through VIF. The "final branch" is that in contact or adjacent to the PPNs on navigation CT. OR =odds ratio; CI = confidence interval; VIF = variance inflation factor; PPNs = peripheral pulmonary nodules; CT = computed tomography.

https://dx.doi.org/10.21037/tlcr-2026-1-0133

Table S4 Group differences for airway geometrical features

Branch level	Variables	Easily accessible (N=182)	Difficult or inaccessible (N=37)	P value
Total branches	Total sectional length, mm	232.15 ± 31.11	226.15 ± 30.85	0.285
	Total Sum of bifurcation angle-in, degree	182.45 ± 44.38	201.93 ± 44.58	0.021
	Total Min of bifurcation angle-in, degree	16.18 ± 7.90	17.78 ± 7.27	0.258
	Total Max of bifurcation angle-in, degree	48.28 ± 8.79	54.34 ± 19.76	0.003
	Total Average of bifurcation angle-in, degree	31.61 ± 6.18	35.23 ± 9.12	0.003
	Total SD of bifurcation angle-in, degree	12.39 ± 4.15	14.63 ± 10.88	0.034
Previous branch to final branch	Sectional length, mm	14.43 ± 6.04	12.57 ± 7.04	0.099
	Bifurcation angle-in, degree	28.52 ± 12.73	32.04 ± 12.54	0.126
	Min sectional area, mm^2	29.01 ± 21.29	31.15 ± 30.71	0.609
	Max sectional area, mm^2	180.78 ± 184.02	229.04 ± 445.6	0.280
	Average sectional area, mm^2	69.27 ± 52.40	71.67 ± 67.94	0.810
	Min of max inscribed sphere R, mm	2.32 ± 0.55	2.26 ± 0.75	0.536
	Max of max inscribed sphere R, mm	3.19 ± 0.90	3.00 ± 1.12	0.278
	Max of min diameter, mm	8.91 ± 4.53	8.79 ± 6.33	0.892
	Max of max diameter, mm	26.73 ± 14.45	30.57 ± 24.34	0.198
	Min of min–max diameter ratio	0.26 ± 0.09	0.22 ± 0.08	0.021
	Max of min–max diameter ratio	0.86 ± 0.12	0.85 ± 0.15	0.685
	Average of min–max diameter ratio	0.57 ± 0.11	0.55 ± 0.13	0.360
	Max curvature, mm^{-1}	0.35 ± 0.12	0.35 ± 0.12	0.787
	Average curvature, mm^{-1}	0.14 ± 0.04	0.14 ± 0.04	0.859
	Min torsion, mm^{-1}	-1.56 ± 2.24	-1.33 ± 1.31	0.555
	Max torsion, mm^{-1}	1.71 ± 2.35	1.64 ± 1.48	0.856
	Average torsion, mm^{-1}	0.02 ± 0.30	0.05 ± 0.31	0.656
	Min perimeter, mm	19.46 ± 7.18	19.28 ± 8.42	0.888
	Max perimeter, mm	71.47 ± 45.34	74.48 ± 49.06	0.717
	Min luminal circularity	0.61 ± 0.12	0.59 ± 0.12	0.418
	Max luminal circularity	1.32 ± 0.40	1.31 ± 0.34	0.880
	Average luminal circularity	0.88 ± 0.09	0.88 ± 0.11	0.778
	Max hydraulic luminal diameter, mm	14.79 ± 11.96	14.95 ± 12.14	0.942
	Average hydraulic luminal diameter, mm	7.26 ± 2.74	7.23 ± 3.37	0.944
Final branch	Sectional length, mm	26.05 ± 14.20	29.54 ± 15.25	0.181
	Bifurcation angle-in, degree	25.65 ± 125.60	31.19 ± 24.49	0.045
	Min sectional area, mm^2	13.93 ± 10.77	11.26 ± 7.11	0.151
	Max sectional area, mm^2	89.85 ± 72.60	91.19 ± 105.16	0.925
	Average sectional area, mm^2	31.42 ± 20.61	26.31 ± 21.15	0.173
	Min of max inscribed sphere R, mm	1.67 ± 0.30	1.57 ± 0.28	0.058
	Average of max inscribed sphere R, mm	2.01 ± 0.31	1.87 ± 0.34	0.018
	Max of min diameter, mm	7.46 ± 3.37	7.12 ± 3.05	0.566
	Min of min–max diameter ratio	0.29 ± 0.09	0.29 ± 0.09	0.849
	Max of min–max diameter ratio	0.91 ± 0.12	0.92 ± 0.11	0.368
	Average of min–max diameter ratio	0.64 ± 0.11	0.66 ± 0.11	0.173
	Max curvature, mm^{-1}	0.50 ± 0.14	0.56 ± 0.17	0.017
	Average curvature, mm^{-1}	0.20 ± 0.04	0.22 ± 0.05	0.032
	Min torsion, mm^{-1}	-2.76 ± 3.00	-2.85 ± 5.80	0.891
	Max torsion, mm^{-1}	2.73 ± 3.98	2.99 ± 2.90	0.707
	Average torsion, mm^{-1}	-0.005 ± 0.27	0.05 ± 0.30	0.262
	Min perimeter, mm	49.25 ± 39.99	58.71 ± 73.24	0.267
	Max perimeter, mm	0.65 ± 0.11	0.64 ± 0.13	0.498
	Min luminal circularity	1.03 ± 0.22	0.97 ± 0.04	0.069
	Max luminal circularity	0.88 ± 0.06	0.89 ± 0.05	0.503
	Average luminal circularity	3.61 ± 0.87	3.34 ± 0.82	0.085
	Max hydraulic luminal diameter, mm	8.53 ± 5.70	6.61 ± 1.69	0.043
	Average hydraulic luminal diameter, mm	4.98 ± 1.30	4.41 ± 0.89	0.010

https://dx.doi.org/10.21037/tlcr-2026-1-0133

References

29. Gonzalez AV, Silvestri GA, Korevaar DA, et al. Assessment of Advanced Diagnostic Bronchoscopy Outcomes for Peripheral Lung Lesions: A Delphi Consensus Definition of Diagnostic Yield and Recommendations for Patient-centered Study Designs. An Official American Thoracic Society/American College of Chest Physicians Research Statement. Am J Respir Crit Care Med 2024;209:634-46.

https://dx.doi.org/10.21037/tlcr-2026-1-0133